

Supporting Information for

“The Effect of Magnesium Substitution on the Hardness of Synthetic and Biogenic Calcite”

Miki E. Kunitake, Shefford P. Baker,* Lara A. Estroff*

Department of Material Science & Engineering, Cornell University, Ithaca, NY 14853

*Email: spb14@cornell.edu; lae37@cornell.edu

The supplemental materials contain:

- I. Supplemental Figures
 - a. **Figure S1:** Representative surface scan prior to indentation
 - b. **Figure S2:** Graphical representation of WDS data
 - c. **Figure S3:** Indentation modulus data

- II. Detailed Experimental Methods
 - a. Geologic calcite specimen preparation
 - i. **Figure S4:** Conoscopic image showing orientation of crystal
 - b. Magnesium-containing calcite specimen preparation
 - i. **Figure S5:** Optical image of cubic zirconia
 - c. Nanoindentation
 - d. Wavelength Dispersive Spectroscopy (WDS)
 - e. Scanning Electron Microscopy (SEM)
 - f. Correlation of WDS and nanoindentation measurements

I. Supplemental Figures

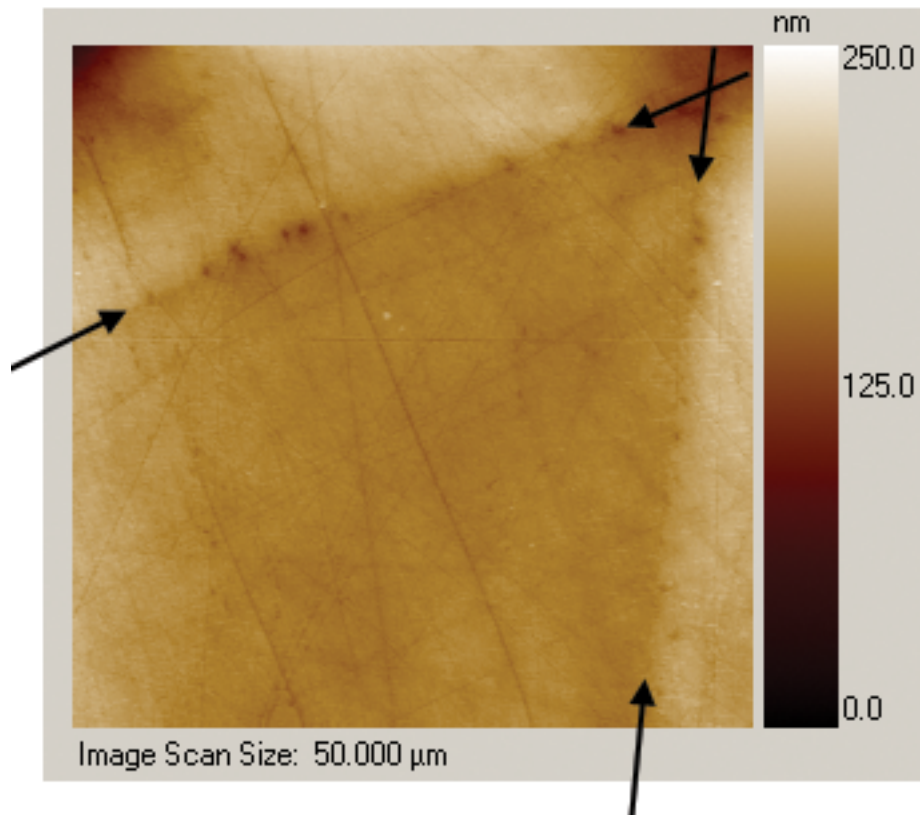


FIG. S1. Surface topography of seed calcite crystal and magnesium-containing overgrowth as scanned by nanoindenter tip prior to indentation. The arrows indicate the interface between seed crystal and overgrowth.

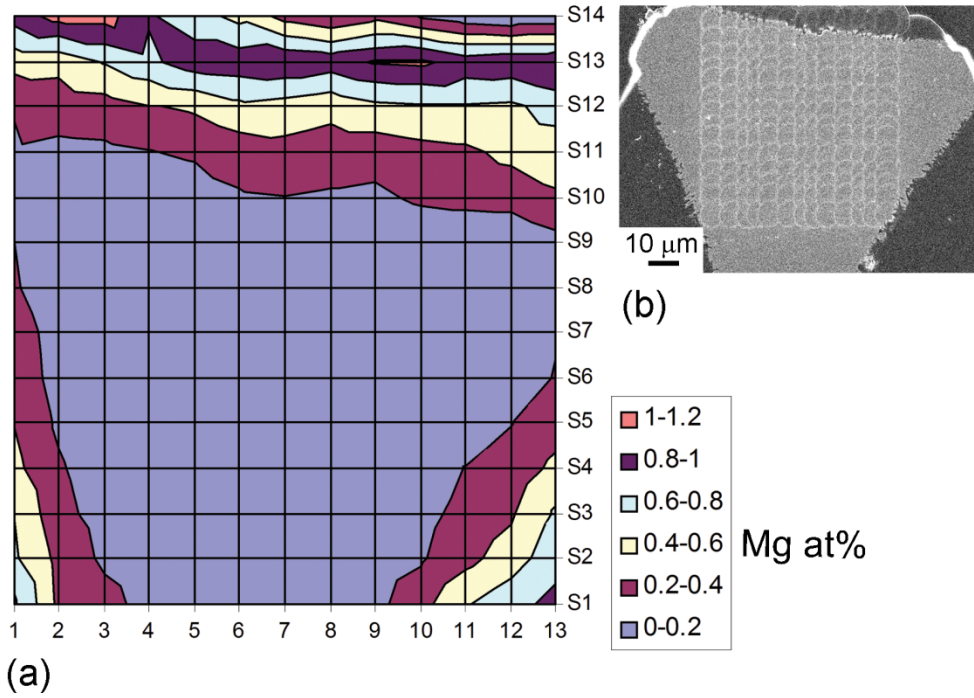


FIG. S2. (a) Graphical representation of WDS magnesium data, with each square representing a 5 μm spot. The Mg-free seed crystal (light purple) is clearly seen in the center, surrounded by growth-bands of equal Mg-content. (b) SEM image taken with in-lens detector showing location of WDS measurements.

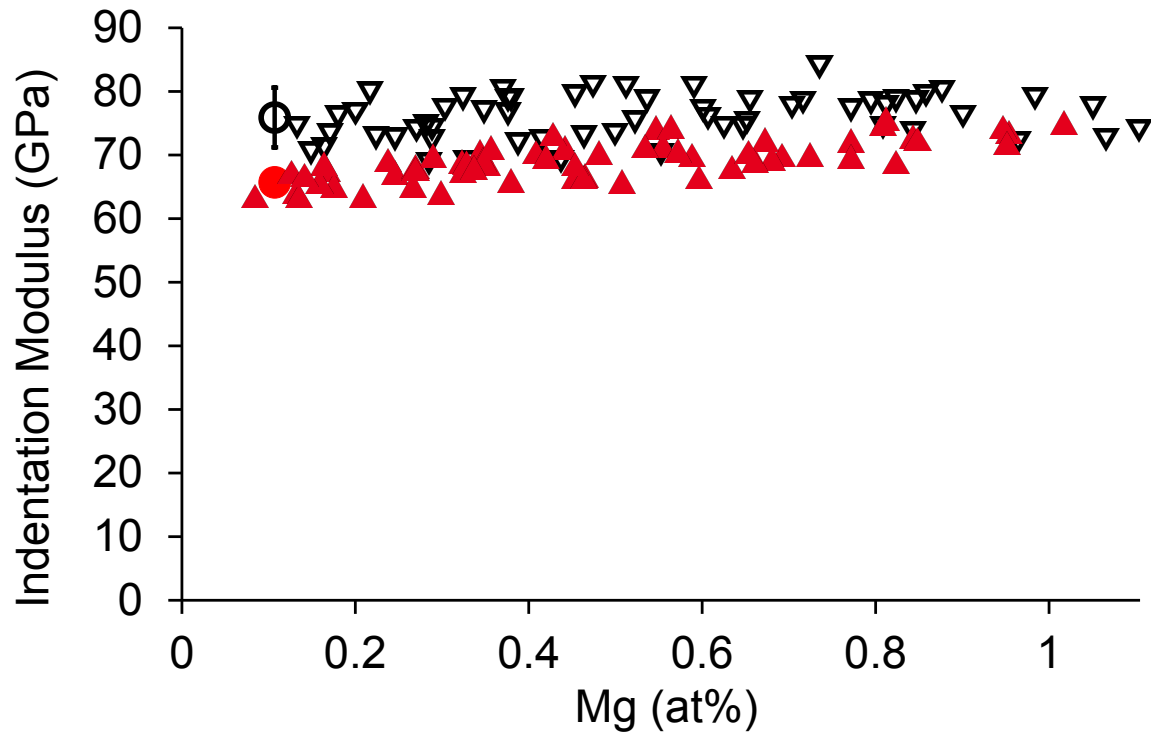


FIG. S3. Plane strain indentation modulus,^{1,2} as a function of Mg-content in overgrowth region. Triangles represent 0° (open black) and 60° (filled red) azimuthal angles while correspondingly colored circles represent the reference geologic values. For a standard fused silica sample, the plane strain indentation modulus was 74.95 ± 1.25 GPa (n=4).

II. Experimental Methods

Geologic calcite specimen preparation: An optically clear geologic calcite rhombohedron (1-2 cm in length) was polished to expose the (001) plane (Iceland spar, Carolina Biological Supplies GEO3429B). The sample was first manually polished by hand on a 30 μm aluminum oxide lapping film until $\sim 1 \text{ cm}^2$ of both the (001) and (00-1) planes were exposed. Rough adjustments to the crystallographic orientation were made by polishing both {001} faces of the crystal until the vertex of each corner of the exposed surfaces were within a few degrees of an equilateral triangle as measured on a rotating microscope stage. Fine adjustments were then made by using a conoscope and centering the interference pattern or isogyre. The interference pattern was viewed with a Leica DM EP polarizing microscope set up as a conoscope by removing the eyepiece (Figure S4). We were able to orient the c axis to within $\sim 1^\circ$ of the surface normal using this technique. The crystal was then fixed with a cyanoacrylate resin (instant Krazy Glue, Elmers) to a glass microscope slide and the exposed (001) face was polished with a graded set of aluminum oxide lapping films followed by a final polish with a 50 nm Al_2O_3 powder (Buehler micropolish $\gamma\text{-Al}_2\text{O}_3$) suspended in a water and 2-methyl-2,4-pentanediol mix (Green Lube, Allied High Tech).²

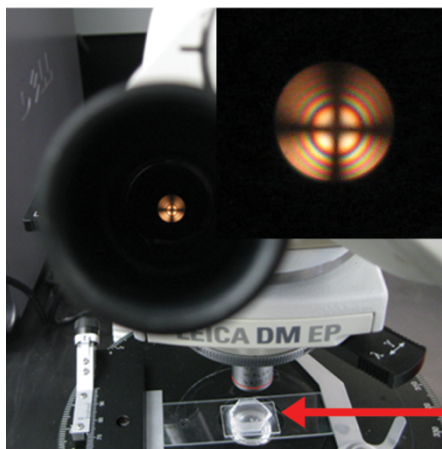


FIG. S4. Experimental setup used during polishing to orient a geologic calcite crystal. Interference pattern (inset) is centered when the optical axis (c axis) is vertical. The field of view is $\sim 8^\circ$. The red arrow points to the geologic crystal, visible at the bottom of the image beneath the microscope objective.

Magnesium-containing calcite specimen preparation: A gradient of magnesium content in calcite was epitaxially overgrown on seed crystals, which were oriented by gravity to rest in aluminum impressions such that the c axis of the crystals was normal to the surface.

Substrate preparation: An array of impressions $\sim 60 \mu\text{m}$ deep were made in 1/16 inch thick marine corrosion resistant aluminum 5052 (Speedy Metals) by using a home-built indenter that mimicked the morphology of the calcite rhombohedron. The home-built cubic zirconia indenter was polished using an Imahashi crystal polisher (Faceting Unit Model FAC-8) to orient the cubic zirconia at the desired angles and polished with a

graded set of aluminum oxide lapping films. The crystal polisher is accurate to within 1° and it is estimated from light microscopy that the radius of curvature of the tip of the cubic zirconia was $\sim 3 \mu\text{m}$ (Figure S5). The polished crystal was then attached perpendicularly to the knife mount of a Sorvall MT 2B ultramicrotome and the manual stepper of the microtome was used to press the cubic zirconia indenter into the aluminum substrate. A 4 by 11 array of impressions with $300 \mu\text{m}$ spacing was made, using the microtome's stage micrometers to reposition the indenter between impressions.

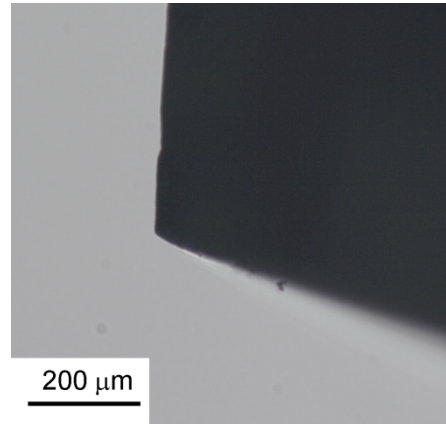


FIG. S5. Optical microscope image of home-built cubic zirconia indenter, polished to be geometrically similar to a calcite rhombohedron. The indenter is used to make oriented impressions in aluminum that then hold the seed crystals.

Seed crystal growth: The seed crystals were grown in agarose gels according to our previously published procedure.³ Briefly, CO_2 gas (from the sublimation of ammonium carbonate) was diffused into a hydrogel containing 1 w/v % agarose (Type IB; Sigma) and 5 mM CaCl_2 . After overnight growth, the crystals were extracted by melting the hydrogel in boiling water until the crystals settled to the bottom of the container. The supernatant was then decanted and the crystals rinsed once with water and once with ethanol. This growth method creates relatively large ($\sim 75 \mu\text{m}$ on edge) and uniform seed crystals that are large enough to be manipulated under a dissecting microscope.

Mg-containing calcite overgrowth: The aluminum specimen holder was placed in a 15 mm petri dish with 3 mL of a solution of 1 mM MgCl_2 ($\text{MgCl}_2 \cdot 6\text{H}_2\text{O}$; Sigma Aldrich 99%) and 5 mM CaCl_2 ($\text{CaCl}_2 \cdot \text{H}_2\text{O}$; Strem Chemicals 99.999%). Approximately 50 to 100 seed crystals were placed on top of the aluminum specimen holder. The crystals were then manually pushed into the impressions using a glass fiber $\sim 50 \mu\text{m}$ in diameter that was drawn by hand from a pipette. Gravity aligns the crystals in the impressions once they are close to the right orientation. Using the ammonium carbonate diffusion method, the seed crystals were then overgrown for 10 days to ensure adequate overgrowth and sufficient binding to the substrate. After overgrowth, the crystals were gently rinsed with DI water followed by ethanol to ensure their binding to the substrate and to clean the surface. Cyanoacrylate resin (instant Krazy Glue, Elmers) was then poured over the top of the array to embed the crystals. We then polished through the resin to expose the seed crystals and magnesium-containing calcite overgrowth using a graded set of aluminum oxide lapping films ending with a 50 nm Al_2O_3 powder (Buehler micropolish $\gamma\text{-Al}_2\text{O}_3$)

suspended in a water and 2-methyl-2,4-pentanediol mix (Green Lube, Allied High Tech).² Surface roughness as measured by the nanoindenter surface scan was less than 10 nm RMS (Figure S1).

Nanoindentation: Load-displacement measurements were performed using a commercial nanoindenter system (Hysitron Triboindenter, Minneapolis, MN) in quasistatic mode. Prior to data collection, the tip shape of a Berkovich diamond indenter with a tip radius of ~120 nm was calibrated using the procedure of Oliver and Pharr.⁴ Each indent consisted of five second load, hold and unload segments with the unloading segment used to calculate the plane strain indentation modulus and hardness via the method of Oliver and Pharr.⁵ A 5 by 5 array of indents with 10 μm spacing was made in the overgrowth region of each crystal at 0° and 60° azimuthal angles (where we define the azimuthal angle to be 0° when the faces of the Berkovich tip, the {001} surface, and the adjacent {104} facets share common zone axes).² A total of 5 crystals were examined.

Wavelength Dispersive Spectroscopy (WDS): WDS measurements were done after nanoindentation to ensure any surface damage induced by WDS was not reflected in the hardness measurements. WDS measurements were done using a JEOL 8900 microprobe with a 5 μm spot size, 6.5 nA current, 10 kV accelerating voltage, and 30 second acquisition time. The samples were coated in a thermal evaporator with ~25 nm of amorphous carbon to reduce charging. Magnesium and calcium content were calibrated against diopside ($\text{MgCaSi}_2\text{O}_8$) and calcite standards, respectively. An ~10 by 15 array of measurements with ~5 μm spacing was used for each crystal. WDS data were collected from the same 5 crystals that were used to determine hardness. For *Atrina rigida* (Gulf Specimen Marine Lab, Florida) and the geologic sample (Iceland spar), magnesium content was determined at 48 points in 43 prisms and at 32 points in one geologic single crystal, respectively.

Scanning Electron Microscopy (SEM): A scanning electron microscope (LEO 1550 FESEM) was used to characterize the location of the indentation and WDS measurements. Using the secondary electron detector, it was possible to see the location of the indents. Using the in-lens detector, which captures both backscattered and secondary electrons, we were able to see the location of the WDS imprints (Figure S2b).

Correlation of WDS and nanoindentation measurements: We then pieced together higher magnification images and measured the distance between the edge of the crystal and the center of the indents or WDS imprints from the images. We then fit a third order polynomial to the cumulative WDS data and used this polynomial to determine the magnesium content at the nanoindentation locations.

References:

1. M.E. Broz, R.F. Cook and D.L. Whitney: Microhardness, toughness, and modulus of Mohs scale minerals. *Am. Mineral.* **91**, 135 (2006).
2. M.E. Kunitake, L.M. Mangano, J.M. Peloquin, S.P. Baker and L.A. Estroff: Evaluation of strengthening mechanisms in calcite single crystals from mollusk shells. *submitted* (2012).
3. H.Y. Li and L.A. Estroff: Calcite growth in hydrogels: assessing the mechanism of polymer-network incorporation into single crystals. *Adv. Mater.* **21**, 470 (2009).
4. W.C. Oliver and G.M. Pharr: Measurement of hardness and elastic modulus by instrumented indentation: advances in understanding and refinements to methodology. *J. Mater. Res.* **19**, 3 (2004).
5. W.C. Oliver and G.M. Pharr: An improved technique for determining hardness and elastic modulus using load and displacement sensing indentation experiments. *J. Mater. Res.* **7**, 1564 (1992).